Sendai Virus Infection Induces Expression of Novel RNAs in Human Cells

Roli Mandhana, Curt M. Horvath*

Department of Molecular Biosciences

Northwestern University, Evanston, IL 60208, USA

*Corresponding author

Tel: (847) 491-5530

Fax: (847) 491-0848

Email: horvath@northwestern.edu

Abstract

Innate antiviral immune responses are driven by virus-induced changes in host gene expression. While much research on antiviral effectors has focused on virus-inducible mRNAs, recent genome-wide analyses have identified hundreds of novel target sites for virus-inducible transcription factors and RNA polymerase. These sites are beyond the known antiviral gene repertoire and their contribution to innate immune responses is largely unknown. In this study, RNA-sequencing of mock-infected and Sendai virus-infected cells was performed to characterize the virus-inducible transcriptome and identify novel virus-inducible RNAs (nviRNAs). Virus-inducible transcription was observed throughout the genome resulting in expression of 1755 previously RefSeq-annotated RNAs and 1545 nviRNAs. The previously-annotated RNAs primarily consist of protein-coding mRNAs, including several well-known antiviral mRNAs that had low sequence conservation but were highly virus-inducible. The previously-unannotated nviRNAs were mostly noncoding RNAs with poor sequence conservation. Independent analyses of nviRNAs based on infection with Sendai virus, influenza virus, and herpes simplex virus 1, or direct stimulation with IFNα revealed a range of expression patterns in various human cell lines. These phylogenetic and expression analyses suggest that many of the nviRNAs share the high inducibility and low sequence conservation characteristic of well-known primary antiviral effectors and may represent dynamically evolving antiviral factors.

Introduction

Virus infection of human cells initiates host cell signaling cascades that result in widespread changes in gene expression. Collectively, these changes produce robust antiviral responses that form the basis of innate and adaptive immunity[1,2]. Induction of the immune response depends on recognition of viral components by host pattern recognition receptors. Though RNA- and DNA-genome viruses are detected by distinct pattern recognition receptors[3,4], the cellular response to most virus infections culminates in the activation of master transcription factors IRF3 and NF-κB.

The most widely studied virus-induced RNAs encode effector proteins that mediate virus interference and signal amplification[5], including several types of interferon (IFN), antiviral cytokines that are secreted from the infected cells[6]. Type I IFN includes the single IFNβ, as well as a number IFNα subtypes that all bind to a common IFNα/β receptor[6]; Type II IFN includes the single IFNγ that binds to the distinct IFNγ receptor[6]; Type III IFN includes IFNλ members, also known as IL-28 and IL-29, that bind to a distinct IFNλ receptor[7]. These receptors activate downstream JAK-STAT signaling[8,9] and the expression of hundreds of effectors, known as interferon stimulated genes (ISGs)[10-12].

The rise in genome-wide sequencing studies has revealed many previously unrecognized RNA species including noncoding RNAs with diverse roles in cellular processes such as gene expression, post-transcriptional regulation, translation, cell cycle regulation, and immune responses[13-17]. Noncoding RNAs are also increasingly

being linked to the cellular response to viruses. For example, BISPR is an IFNα-induced long noncoding RNA (lncRNA) that regulates the expression of tetherin, a cellular antiviral factor that blocks viral release[18,19]. NEAT1 is a virus-induced lncRNA that regulates the expression of antiviral genes such as IL-8[20]. In the case of lncRNA-ACOD1, expression promotes rather than interferes with virus replication by regulating cellular metabolism[21]. These examples underscore the importance of deep sequencing approaches to characterize the extent of noncoding RNA transcription following virus infections.

Our previous study in human cells showed that early responses to RNA-genome virus infections initiate genome-wide binding of IRF3 and NF-κB to diverse loci to recruit and activate RNA polymerase II, assemble transcriptional machinery, and induce transcription[22]. Many of these binding sites were novel virus-inducible sites in intergenic and intronic regions of the genome, suggesting the existence of novel virus-inducible RNAs[22]. The identification of these novel binding sites along with the recent increase in identification of individual novel RNAs with functions related to regulation of virus infection motivated genome-wide examination of virus-inducible RNAs. In this study, novel RNA-encoding loci were identified throughout the genome, but unlike most annotated RNAs, they were primarily expressed from intergenic regions. Analysis of newly-identified virus-induced RNAs, referred to here as nviRNAs[22], reveals that they can be induced by RNA and DNA-genome viruses as well as by direct stimulation with the type I IFN, IFNα, in both general and cell-specific fashion. These findings expand

the extent of virus-induced transcription and suggest that both coding and noncoding RNA expression are hallmarks of the cellular response to virus infections.

Results

RNA-sequencing and identification of differentially expressed genes

To fully appreciate the extent of virus-induced RNA transcription, human Namalwa B cells were infected with Sendai virus, an RNA virus that is a potent inducer of antiviral signaling[22]. Mock-infected cells and cells infected with 5 plaque forming units (pfu) of Sendai virus per cell for 6 hours were subjected to paired-end RNA sequencing. Approximately 200 million reads of 100 bp read length were obtained for each sample. On an average, 90% of total reads mapped to the human reference genome (GRCh37/hg19).

Enrichment of RNAs in mock-infected or virus-infected samples was analysed with the DESeq2 program, resulting in the identification of 6210 RNAs that were differentially expressed after virus infection at a false discovery rate (FDR) of 5% and fold change of at least 1.5. Among these RNAs 3300 were induced by virus infection, while 2910 were suppressed. The expression changes of representative groups of these RNAs were confirmed in independent samples by RT-qPCR using primers specific for virus-induced previously-annotated genes (Fig. 1a) and previously-unannotated RNAs (Fig.1b), as well as for RNAs suppressed by virus infection (Fig. 1c). In all categories, changes in RNA abundance levels measured by RT-qPCR closely matched the expression changes measured in RNA-sequencing analysis.

The magnitude of differential expression was much less for the suppressed RNAs compared to the RNAs induced by virus infection. The expression of the most suppressed RNA, C10orf71, was suppressed only 50-fold by virus infection while the most induced RNA, IL-29, was induced almost 20,000-fold. More than 480 of the virus-induced RNAs are induced by more than 50-fold after virus infection. Due to this discrepancy in range of expression change, further emphasis was placed on analysing the virus-induced RNAs.

Of the 3300 virus-induced RNAs, 1755 have an existing RefSeq annotation[23]. The most highly induced of these annotated RNAs (Table 1) code for proteins known to play key roles in the cellular response to viruses, including type I IFNs[6] (IFNβ, IFNα8, and IFNα13), type III IFNs[7] (IL-29, IL-28α and IL28β), chemokines[24] (CXCL10 and CXCL11), the antiviral mediator, OASL[25], and the antiviral E3 ligase, HERC5[26,27]. In addition, 115 of the 389 previously identified type I ISGs compiled in a recent study[28] were found to be induced by at least 1.5 fold.

Gene enrichment analysis

To further characterize these induced RNAs, cellular pathways induced by virus infection were identified using DAVID Bioinformatics Resources[29,30], a functional annotation tool that determines statistically significant gene enrichment in biological processes from a given gene list. The previously-annotated virus-induced RNAs mapped to 1608 DAVID gene IDs and were significantly enriched in more than 400

Gene Ontology (GO) biological processes and 40 Kyoto Encyclopedia of Genes and Genomes (KEGG) pathways.

As expected, the top 10 most enriched GO processes describe cellular functions that enable the cell to respond to virus infection, including type I IFN and cytokine signaling (Fig. 2a). The top 10 most enriched KEGG pathways also describe pathways in response to various RNA viruses such as influenza A virus, measles virus, and hepatitis C virus, a DNA virus, herpes simplex virus, and several pattern recognition receptor pathways including toll-like receptor signaling, RIG-I-like receptor signaling, and cytosolic-DNA sensing (Fig. 2b).

To better understand the extent of biological processes that are induced after virus infection, clustering analysis was carried out on all enriched GO biological process terms. The enriched GO biological processes formed 27 clusters with an enrichment score above 3, indicating that a majority of the processes within the cluster were statistically significant (Supplementary Table S1). The top five most enriched clusters relate to type I IFN signaling, cytokine signaling, type II IFN signaling and the unfolded protein response. The IFN and cytokine signaling pathways are known to induce antiviral factors, and the unfolded protein response is a cellular stress response induced by viral protein translation in the host cell. These analyses show that the previously-annotated virus-induced RNAs include many factors with known roles in the cellular response to viruses and that the experimental system used in this study is capable of

uncovering proteins and pathways that are known to be important in the response to viruses.

Genomic distribution of annotated RNAs and nviRNAs

Among the 3300 virus-induced RNAs there were 1755 previously RefSeq-annotated RNAs and 1545 novel virus-inducible RNAs (nviRNAs) that were not previously RefSeq-annotated. The previously-annotated RNAs and the identified nviRNAs were found to be widely distributed among all the chromosomes (Fig. 3a), but the nviRNAs differed from the known RNAs in their distribution among specific genomic features (Fig. 3b). Examination of six genomic feature categories, including: promoters, transcriptional termination sites, coding exons, introns, intergenic regions and untranslated regions (UTRs; includes 5' and 3' UTRs), revealed the majority of annotated RNAs mapped to coding exons (87.6%; Fig. 3b) with fewer than 10% mapping to introns and intergenic regions, indicating that the annotations largely reflect mRNA-encoding genes. In contrast, only 1.7% of the nviRNAs mapped to coding exons while more than 90% mapped to introns or intergenic regions. The finding that most nviRNAs are transcribed from intronic and intergenic regions is consistent with previous work showing abundant virus-induced RNA polymerase II binding and elongation throughout intronic and intergenic regions[22].

Protein coding and conservation analysis of annotated RNAs and nviRNAs

To compare the protein coding potential of the virus-induced RNAs, a PhyloCSF score was calculated for each RNA. PhyloCSF is a method that uses a multi-species

sequence alignment to calculate a score reflecting the likelihood that an open reading frame (ORF) encodes a protein[31]. Analysis of previously characterized RNAs has shown that known noncoding RNAs generally score below 50 while protein-coding genes score above 50[32,33].

There were 10 previously-annotated RNAs and 20 nviRNAs that did not have an ORF and were excluded from this analysis. The remaining 3270 RNAs were analysed and plotted in Fig. 4. Results indicate that the majority of the known RNAs (77.6%, Fig. 4a) were predicted to be protein coding mRNAs, while only 4.2% of the nviRNAs were predicted to encode a protein (Fig. 4a). Similar results were seen when limiting to RNAs induced at least 5-fold by virus infection (Supplementary Fig. S1). Of the previously-annotated RNAs, 69.6% were predicted to encode a protein while only 2.2% of the nviRNAs were likely to be protein coding. However, for both the previously-annotated RNAs and the nviRNAs, a larger proportion of the RNAs mapping to exonic genomic features had a high PhyloCSF score (Fig. 4b-c). For the annotated RNAs, 87% of the RNAs mapping to exons had a PhyloCSF score greater than 50 (Fig. 4b). Similarly, 52% of the nviRNAs mapping to exons had a PhyloCSF score above 50 (Fig. 4c). These results indicate that the nviRNAs are mostly virus-inducible noncoding RNAs, but there are 64 nviRNAs that were identified to have protein-coding potential.

Though the nviRNAs are mostly noncoding RNAs, they may nevertheless have important functions in the antiviral system. Sequence conservation among vertebrates is frequently used to determine functional capacity of RNAs. However, many immune

genes have undergone positive, diversifying selection and are therefore poorly conserved. Lower sequence conservation in virus-inducible genes may be indicative of an important antiviral role.

Sequence conservation among vertebrates was calculated by PhastCons, which uses a multiple-species alignment to calculate a score for each nucleotide corresponding to the probability that it is within a conserved element [34]. To determine average sequence conservation across vertebrates, the mean PhastCons score for each RNA was calculated. Overall, the previously-annotated RNAs had much higher sequence conservation than the nviRNAs (Fig. 4d). While only 50% of the previously-annotated RNAs had a score of 0.413 or less, 98% of the nviRNAs had a score of 0.410 or less, indicating that their sequences were much less conserved than the annotated RNAs. The maximum mean PhastCons score for a nviRNA was 0.687, whereas there were 24 previously-annotated RNAs with scores of 0.9 or higher, suggesting that the nviRNAs on average represent a novel evolving group of RNAs.

Comparison of the PhastCons score with virus-inducibility revealed that the most highly induced previously-annotated RNAs were not highly conserved among vertebrates, in accordance with these genes having evolved under positive selection (Fig. 4e, blue circles). When limiting to RNAs induced at least 5-fold by virus infection, 50% of the previously-annotated RNAs had a score less than 0.343 (Supplementary Fig. S2). The top 10 most up-regulated annotated RNAs all had a mean PhastCons score under 0.5, with the top 5 having a score under 0.3 (Fig. 4e; Table 1). As there were examples of

228 highly-induced nviRNAs that were similarly poorly conserved (Fig. 4f), it is anticipated
229 that at least a fraction of these nviRNAs could have novel functions in the response to
230 viruses.
231
232 **Inducibility of nviRNAs in other conditions**
233 Most of the well-known antiviral genes, including type I IFNs, are broad-acting effectors
234 that are widely induced by diverse viruses and in most cell types. However, there are
235 some antiviral genes that have more restricted antiviral activity[28].
236
237 To determine whether nviRNAs are activated in contexts other than Sendai virus
238 infection, a subset of the nviRNAs were screened in Namalwa cells to determine
239 whether their expression could also be induced by infection with two viruses identified
240 through the KEGG pathways (Fig. 2): a distinct RNA-genome virus, influenza A virus
241 (A/Udorn/72) and a DNA-genome virus, HSV-1. In addition, cells were subjected to
242 direct stimulation with type I IFN (IFNα). Cells were either infected with 5 pfu/cell of
243 virus for 10 hours or treated with 1000 U/mL IFNα for 6 hours prior to RNA isolation for
244 gene expression analysis by RT-qPCR with gene-specific primers. The known virus-
245 induced genes IFIT1[35], IFNβ[6], CSAG3 and USP18[36] were used as controls. This
246 analysis revealed great variation in the inducibility of the nviRNAs, not only in which
247 stimuli induced them, but also in the level of induction (Fig. 5; Supplementary Table S2).
248 Using a 2-fold increase in expression as a minimum for induction, the nviRNAs were
249 classified into one of eight clusters based on their behavior (Fig. 5): (1) inducible by
250 viruses and IFNα, (2) inducible by viruses only, (3) inducible by RNA-viruses and IFNα,

(4) inducible by RNA viruses only, (5) inducible by Sendai virus and HSV-1 as well as IFNα, (6) inducible by both Sendai virus and HSV-1, (7) inducible by Sendai virus and IFNα, and (8) inducible by influenza A virus or HSV-1. The nviRNAs that were inducible by multiple viruses and IFNα may represent type I ISGs that are broad-acting novel antiviral effectors, while the nviRNAs induced by a subset of stimuli may represent restricted antiviral effectors.

To investigate the cell-specificity of these nviRNA transcriptional responses, the inducibility after virus infection and IFNα stimulation was also examined in several other human cell types. The epithelial 2fTGH cells and monocyte THP-1 cells were infected with 5 pfu/cell of Sendai virus (for 4 hours due to cytopathic effects) or influenza A virus (10 hours) or directly treated with IFNα (6 hours). THP-1 cells were also infected with 5 pfu/cell of HSV-1 (10 hours). In 2fTGH cells, transfection of the synthetic dsRNA, poly(I:C), an IFN activator that can robustly induce the expression of IFNs and ISGs, was included as a stimulus. The known virus-induced genes IFNβ[6], IFIT1[35], CSAG3 and USP18[36] were expressed in both 2fTGH cells (Fig. 6a) and THP-1 cells (Fig. 7a) by various stimuli. The 6 nviRNAs identified as most likely to be broad-acting antiviral effectors in the Namalwa cells screen were also induced in both 2fTGH cells (Fig. 6b) and THP-1 cells (Fig. 7b). In 2fTGH cells, all the tested nviRNAs were induced by poly(I:C), though XLOC_035959 was induced less than 2-fold (Fig. 6b). Expression of the other 5 nviRNAs was also up-regulated more than 2-fold by influenza A virus. In THP-1 cells, influenza A virus robustly induced all 6 nviRNAs (Fig. 7b), with HSV-1 and IFNα also inducing half of the tested nviRNAs. The expression of the nviRNAs in the

cluster only inducible by viruses in Namalwa cells was also tested in other cell types. There was greater variability in the inducibility of these nviRNAs. There were 6 nviRNAs induced in both 2fTGH cells (Fig. 6c) and THP-1 cells (Fig. 7c) by 10 hours of influenza A virus infection, while the other 5 nviRNAs showed more varied induction (Table 2).

The expression level and induction of each nviRNA varied greatly depending on the inducing stimulus, likely due to differences in the activation kinetics or intensity of each stimulus. Of the 12 nviRNAs expressed in both 2fTGH cells and THP-1 cells, 10 nviRNAs were also expressed in the epithelial HeLa and A549 cells (Table 2, Supplementary Table S3). The expression of these nviRNAs by at least 1 stimulus, and in most cases more than 1 stimulus, in multiple cell types demonstrates that these nviRNAs are not cell-specific and are candidates for antiviral function.

Discussion

In this study, RNA-sequencing of Namalwa cells mock-infected or infected with Sendai virus identified 1755 previously RefSeq-annotated RNAs and 1545 novel virus-inducible RNAs (nviRNAs). Analysis of these virus-inducible RNAs revealed insights into the previously unrecognized depth and breadth of the virus-inducible transcriptome, and identified nviRNAs as possible targets of positive selection in the cellular response to viruses.

296 This study was motivated in part by the identification of novel virus-inducible binding
297 sites for the antiviral transcription factors IRF3 and NF-κB, and RNA polymerase II[22].
298 Based on the RNA polymerase II binding sites, 1450 nviRNAs were predicted to be
299 expressed[22]. Using the same cell line and virus for infection, 501 of these predicted
300 nviRNAs were partially matched to RNAs identified in RNA-sequencing analysis.
301 Factors that may contribute to this apparent disparity include timing, abundance and
302 methodology. Furthermore, most of these RNAs were excluded from further analysis
303 due to their low expression levels. Nevertheless, since many noncoding RNAs have
304 low expression levels[37], the subset of functional nviRNAs may extend past the 1545
305 nviRNAs analysed in this study.
306
307 Though both previously-annotated RNAs and nviRNAs were distributed similarly across
308 the chromosomes (Fig. 3a), there was a significant difference in the genomic features
309 associated with these different loci. More than 80% of the previously-annotated RNAs
310 were transcribed from exons, whereas more than 80% of the nviRNAs were transcribed
311 from intergenic regions (Fig. 3b). Even when limiting to RNAs with a high PhyloCSF
312 score, indicating a strong likelihood that the RNA encodes a protein, 96.4% of the
313 previously-annotated RNAs and only 21.8% of the nviRNAs mapped to exons. This
314 discrepancy highlights that current annotations of genomic features are based on
315 identification of a relatively small number of RNAs and the labeling of most of the
316 genome as intergenic “junk” DNA. The recent expansion in sequencing studies that
317 identify novel RNAs indicates a need for a corresponding refinement in annotations of
318 genomic features.

The protein coding potential and functionality of the virus-inducible RNAs was assessed using PhyloCSF and PhastCons respectively. A majority of the previously RefSeq-annotated RNAs were identified as protein coding mRNAs, while very few of the nviRNAs were found likely to encode a protein (Fig. 4). The mean PhastCons score of each RNA was used to determine its average conservation. Though the previously-annotated RNAs vary in their mean PhastCons score, the most highly inducible, well-known RNAs that encode antiviral factors had a PhastCons score below 0.5 (Fig. 4e; Table 1), indicating low conservation may be suggestive of positive selection and overall importance to the cellular response to viruses.

While most genes have undergone negative selection to be conserved through evolution, many immune genes have been positively selected for diversity[38,39]. Virus evolution to overcome host antiviral immunity creates a potent selective force for diversification of key antiviral effectors. The cyclical virus-host interplay has resulted in immune genes being among the more recently evolved and more diversified genes in the human genome[40]. The poor sequence conservation of the highly induced nviRNAs may indicate that they are previously unidentified antiviral factors that evolved under positive selection.

In further support of this concept of nviRNA functionality, expression of a subset of nviRNAs was analysed and found to be induced, albeit variably, by different RNA and DNA viruses, and antiviral stimulation with poly(I:C) and IFNα. Differences in both

342 expression and temporal regulation were observed among the nviRNAs tested due to
343 specific virus or treatment, as well as in the cellular host cell line. It is reasonable to
344 speculate that at least some of the nviRNAs, particularly the 10 expressed in 5 different
345 cell lines tested (Fig. 5, Table 2), could represent novel antiviral factors with unique
346 roles in the cellular innate immune response to viruses. This expression analysis does
347 not assign any specific function to these novel RNAs, but their identification and
348 classification is the first step in understanding their roles in the cellular response to virus
349 infections. A loss of function analysis should be conducted for the nviRNAs that were
350 classified as inducible in multiple cell lines to determine their function.
351
352 This study focused on identifying nviRNAs with potential functions in the cellular
353 response to viruses; however, it is worthwhile to also examine potential novel antiviral
354 factors among the previously RefSeq-annotated RNAs. Many of these RNAs encode
355 known antiviral genes that are enriched in critical antiviral biological processes, but not
356 all of the annotated RNAs have been assigned an antiviral function. Of the 1755
357 previously-annotated virus-induced RNAs, 328 were not assigned to any GO biological
358 process, indicating that they are poorly characterized functionally. Additionally, there
359 are many RNAs that despite being assigned a GO biological process, were not
360 previously identified as virus-inducible RNAs. Combining these previously-annotated,
361 virus-inducible RNAs with the nviRNAs identifies a large pool of potential antiviral
362 responders that could have untapped value as antiviral diagnostic or therapeutic tools.
363

364 ## Materials and Methods

365 *Cells, Viruses, and Treatments*

366 Namalwa B cells (ATCC CRL-1432) and THP-1 cells (ATCC TIB-202) were cultured in
367 RPMI 1640 Medium (Life Technologies, Thermo Fisher Scientific). HeLa cells (ATCC
368 CCL-2), A549 cells (ATCC CCL-185) and 2fTGH cells (ECACC 12021508) were
369 cultured in Dulbeco's Modified Eagle Medium (Life Technologies, Thermo Fisher
370 Scientific). For all cell lines medium was supplemented with 10% Cosmic calf serum
371 (HyClone, GE Healthcare Life Sciences) and 1% Penicillin-Streptomycin (Gibco,
372 Thermo Fisher Scientific). Sendai virus (Cantell strain) was grown in embryonated
373 chicken eggs, and titers were determined on Vero cells. The A/Udorn/72 strain of
374 influenza virus (gift of R. A. Lamb, Northwestern University) was propagated and titer
375 was determined on MDCK cells. HSV-1 (F strain) (gift of G. A. Smith, Northwestern
376 University) was propagated and titer was determined on Vero cells. Cells were infected
377 at a multiplicity of infection (MOI) of 5 for indicated times. Virus infections were
378 performed in serum-free medium (SFM), with 1% bovine serum albumin (BSA)
379 supplemented for influenza virus. At 1 hour post-infection, the inoculation medium was
380 replaced with medium containing 2% serum for the remainder of the infection. For
381 poly(I:C) transfection, 2.5 μg/mL of low and high molecular weight poly(I:C) (Invivogen)
382 was transfected for 6 hours using the Lipofectamine 2000 (Invitrogen, Thermo Fisher
383 Scientific) transfection reagent. For direct treatment with IFNα, cells were treated with
384 1000 U/mL recombinant IFNα (Roche).

385

386 *Total RNA Extraction*

Total RNA was extracted using the TRIzol Reagent (Invitrogen, Thermo Fisher Scientific) and treated with DNAse I (Invitrogen, Thermo Fisher Scientific). The RNA quantity was obtained using NanoDrop 2000 (Thermo Fisher Scientific). For RNA used in RNA sequencing, the integrity was examined by the Bioanalyser 2100 system (Agilent Technologies) to obtain RNA Integrity Number (RIN) of over 9.

RNA sequencing and transcript assembly

Duplicate samples of mock-infected and Sendai virus-infected cells for 6 hours were used to prepare RNA libraries for sequencing on Illumina HiSeq2000 platform (Illumina) to generate 100 bp paired-end sequencing reads. Raw data was filtered to remove adapter sequences and low-quality reads. The remaining rRNA reads were removed by mapping to known human rRNA sequences. The clean, high-quality data was mapped to the human reference genome (GRCh37.p10/hg19)[41] using TopHat[42] (2.0.10). The mapped reads for each sample were independently assembled into annotated and novel transcripts using the Cufflinks[43] (2.1.1) suite of programs.

Bioinformatic analysis

To determine differential expression between mock-infected and Sendai virus-infected samples, read counts for each RNA were generated by HTSeq[44] (0.6.0) for each sample and analysed by the DESeq2[45] (1.2.10) program. Significance was calculated using the Wald test and a Benjamini-Hochberg False Discovery Rate cut-off of 5% was used to assess statistically significantly differential expression. The lowest quartile of RNAs based on expression were excluded from further analysis. RefSeq genomic

410 feature distribution information for coding exons, introns, 3' and 5' untranslated regions
411 (UTRs), promoters (-1kb), and transcription termination sites (+1 kb) was downloaded
412 from the UCSC genome browser (http://genome.ucsc.edu/)[23] and analysed using the
413 BEDtools program[46]. The online functional annotation tool, DAVID[29,30] (6.8), was used
414 to conduct gene enrichment analysis. A list of gene symbols corresponding to
415 differentially expressed RNAs was mapped to DAVID gene IDs to determine which
416 Gene Ontology biological processes and KEGG pathways were enriched. A Benjamini-
417 Hochberg False Discovery Rate cut-off of 5% was used to assess statistical
418 significance. Clustering analysis of enriched GO biological processes was done using
419 DAVID's heuristic fuzzy multiple-linkage partitioning method[47]. An enrichment score
420 cut-off of 3 was used to determine significance. Base-by-base PhastCons[34]
421 conservation score across 100 vertebrates were downloaded from the UCSC Genome
422 Browser. For each RNA a mean score was calculated if there was a score available for
423 at least 80% of the bases in the sequence. The PhyloCSF[31] software was locally
424 installed and used to determine the coding potential of the longest start-to-stop open
425 reading frame in each RNA. The multiple-species alignments needed for this analysis
426 were prepared on Galaxy web platform at usegalaxy.org[48].
427
428 *cDNA synthesis and Quantitative PCR*
429 Purified total RNA was random primed and reverse transcribed using SuperScript III
430 Reverse Transcriptase (Invitrogen, Thermo Fisher Scientific). Gene expression was
431 measured by quantitative real-time PCR (qPCR) and normalized to glyceraldehyde 3-
432 phosphate dehydrogenase (GAPDH) to determine relative abundance by the $2^{-\Delta C_T}$

433 method or fold change over mock by the $2^{-\Delta\Delta C}{}_T$ method[49]. Primers are listed in
434 Supplementary Table S4.
435
436 *Data Availability*
437 RNA-sequencing data is available in the GEO database under study GSE115266.
438

439 ## References

440 1 Mogensen, T. H. Pathogen recognition and inflammatory signaling in innate
441 immune defenses. *Clin Microbiol Rev* **22**, 240-273, Table of Contents,
442 doi:10.1128/CMR.00046-08 (2009).
443 2 Takeuchi, O. & Akira, S. Innate immunity to virus infection. *Immunol Rev* **227**, 75-
444 86, doi:10.1111/j.1600-065X.2008.00737.x (2009).
445 3 Kawasaki, T. & Kawai, T. Toll-like receptor signaling pathways. *Front Immunol* **5**,
446 461, doi:10.3389/fimmu.2014.00461 (2014).
447 4 Bruns, A. M. & Horvath, C. M. Antiviral RNA recognition and assembly by RLR
448 family innate immune sensors. *Cytokine Growth Factor Rev* **25**, 507-512,
449 doi:10.1016/j.cytogfr.2014.07.006 (2014).
450 5 Sadler, A. J. & Williams, B. R. Interferon-inducible antiviral effectors. *Nat Rev*
451 *Immunol* **8**, 559-568, doi:10.1038/nri2314 (2008).
452 6 Stark, G. R., Kerr, I. M., Williams, B. R., Silverman, R. H. & Schreiber, R. D. How
453 cells respond to interferons. *Annu Rev Biochem* **67**, 227-264,
454 doi:10.1146/annurev.biochem.67.1.227 (1998).

7 Ank, N., West, H. & Paludan, S. R. IFN-lambda: novel antiviral cytokines. *J Interferon Cytokine Res* **26**, 373-379, doi:10.1089/jir.2006.26.373 (2006).

8 Fu, X. Y., Kessler, D. S., Veals, S. A., Levy, D. E. & Darnell, J. E., Jr. ISGF3, the transcriptional activator induced by interferon alpha, consists of multiple interacting polypeptide chains. *Proc Natl Acad Sci U S A* **87**, 8555-8559 (1990).

9 Kessler, D. S., Veals, S. A., Fu, X. Y. & Levy, D. E. Interferon-alpha regulates nuclear translocation and DNA-binding affinity of ISGF3, a multimeric transcriptional activator. *Genes Dev* **4**, 1753-1765 (1990).

10 Levy, D. E., Kessler, D. S., Pine, R., Reich, N. & Darnell, J. E., Jr. Interferon-induced nuclear factors that bind a shared promoter element correlate with positive and negative transcriptional control. *Genes Dev* **2**, 383-393 (1988).

11 Reich, N. *et al.* Interferon-induced transcription of a gene encoding a 15-kDa protein depends on an upstream enhancer element. *Proc Natl Acad Sci U S A* **84**, 6394-6398 (1987).

12 Der, S. D., Zhou, A., Williams, B. R. & Silverman, R. H. Identification of genes differentially regulated by interferon alpha, beta, or gamma using oligonucleotide arrays. *Proc Natl Acad Sci U S A* **95**, 15623-15628 (1998).

13 Rinn, J. L. & Chang, H. Y. Genome regulation by long noncoding RNAs. *Annu Rev Biochem* **81**, 145-166, doi:10.1146/annurev-biochem-051410-092902 (2012).

14 Guttman, M. & Rinn, J. L. Modular regulatory principles of large non-coding RNAs. *Nature* **482**, 339-346, doi:10.1038/nature10887 (2012).

15 Yoon, J. H., Abdelmohsen, K. & Gorospe, M. Posttranscriptional gene regulation by long noncoding RNA. *J Mol Biol* **425**, 3723-3730, doi:10.1016/j.jmb.2012.11.024 (2013).

16 Fitzgerald, K. A. & Caffrey, D. R. Long noncoding RNAs in innate and adaptive immunity. *Curr Opin Immunol* **26**, 140-146, doi:10.1016/j.coi.2013.12.001 (2014).

17 Djebali, S. *et al.* Landscape of transcription in human cells. *Nature* **489**, 101-108, doi:10.1038/nature11233 (2012).

18 Barriocanal, M., Carnero, E., Segura, V. & Fortes, P. Long Non-Coding RNA BST2/BISPR is Induced by IFN and Regulates the Expression of the Antiviral Factor Tetherin. *Front Immunol* **5**, 655, doi:10.3389/fimmu.2014.00655 (2014).

19 Kambara, H. *et al.* Regulation of Interferon-Stimulated Gene BST2 by a lncRNA Transcribed from a Shared Bidirectional Promoter. *Front Immunol* **5**, 676, doi:10.3389/fimmu.2014.00676 (2014).

20 Imamura, K. *et al.* Long noncoding RNA NEAT1-dependent SFPQ relocation from promoter region to paraspeckle mediates IL8 expression upon immune stimuli. *Mol Cell* **53**, 393-406, doi:10.1016/j.molcel.2014.01.009 (2014).

21 Wang, P., Xu, J., Wang, Y. & Cao, X. An interferon-independent lncRNA promotes viral replication by modulating cellular metabolism. *Science* **358**, 1051-1055, doi:10.1126/science.aao0409 (2017).

22 Freaney, J. E., Kim, R., Mandhana, R. & Horvath, C. M. Extensive cooperation of immune master regulators IRF3 and NFkappaB in RNA Pol II recruitment and pause release in human innate antiviral transcription. *Cell Rep* **4**, 959-973, doi:10.1016/j.celrep.2013.07.043 (2013).

23 Karolchik, D. *et al.* The UCSC Genome Browser database: 2014 update. *Nucleic Acids Res* **42**, D764-770, doi:10.1093/nar/gkt1168 (2014).

24 Groom, J. R. & Luster, A. D. CXCR3 ligands: redundant, collaborative and antagonistic functions. *Immunol Cell Biol* **89**, 207-215, doi:10.1038/icb.2010.158 (2011).

25 Zhu, J., Ghosh, A. & Sarkar, S. N. OASL-a new player in controlling antiviral innate immunity. *Curr Opin Virol* **12**, 15-19, doi:10.1016/j.coviro.2015.01.010 (2015).

26 Wong, J. J., Pung, Y. F., Sze, N. S. & Chin, K. C. HERC5 is an IFN-induced HECT-type E3 protein ligase that mediates type I IFN-induced ISGylation of protein targets. *Proc Natl Acad Sci U S A* **103**, 10735-10740, doi:10.1073/pnas.0600397103 (2006).

27 Dastur, A., Beaudenon, S., Kelley, M., Krug, R. M. & Huibregtse, J. M. Herc5, an interferon-induced HECT E3 enzyme, is required for conjugation of ISG15 in human cells. *J Biol Chem* **281**, 4334-4338, doi:10.1074/jbc.M512830200 (2006).

28 Schoggins, J. W. *et al.* A diverse range of gene products are effectors of the type I interferon antiviral response. *Nature* **472**, 481-485, doi:10.1038/nature09907 (2011).

29 Huang da, W., Sherman, B. T. & Lempicki, R. A. Bioinformatics enrichment tools: paths toward the comprehensive functional analysis of large gene lists. *Nucleic Acids Res* **37**, 1-13, doi:10.1093/nar/gkn923 (2009).

30 Huang da, W., Sherman, B. T. & Lempicki, R. A. Systematic and integrative analysis of large gene lists using DAVID bioinformatics resources. *Nat Protoc* **4**, 44-57, doi:10.1038/nprot.2008.211 (2009).

31 Lin, M. F., Jungreis, I. & Kellis, M. PhyloCSF: a comparative genomics method to distinguish protein coding and non-coding regions. *Bioinformatics* **27**, i275-282, doi:10.1093/bioinformatics/btr209 (2011).

32 Guttman, M. *et al.* Ab initio reconstruction of cell type-specific transcriptomes in mouse reveals the conserved multi-exonic structure of lincRNAs. *Nat Biotechnol* **28**, 503-510, doi:10.1038/nbt.1633 (2010).

33 Guttman, M., Russell, P., Ingolia, N. T., Weissman, J. S. & Lander, E. S. Ribosome profiling provides evidence that large noncoding RNAs do not encode proteins. *Cell* **154**, 240-251, doi:10.1016/j.cell.2013.06.009 (2013).

34 Siepel, A. *et al.* Evolutionarily conserved elements in vertebrate, insect, worm, and yeast genomes. *Genome Res* **15**, 1034-1050, doi:10.1101/gr.3715005 (2005).

35 Pichlmair, A. *et al.* IFIT1 is an antiviral protein that recognizes 5'-triphosphate RNA. *Nat Immunol* **12**, 624-630, doi:10.1038/ni.2048 (2011).

36 Porritt, R. A. & Hertzog, P. J. Dynamic control of type I IFN signalling by an integrated network of negative regulators. *Trends Immunol* **36**, 150-160, doi:10.1016/j.it.2015.02.002 (2015).

37 Derrien, T. *et al.* The GENCODE v7 catalog of human long noncoding RNAs: analysis of their gene structure, evolution, and expression. *Genome Res* **22**, 1775-1789, doi:10.1101/gr.132159.111 (2012).

544 38 Daugherty, M. D. & Malik, H. S. Rules of engagement: molecular insights from
545 host-virus arms races. *Annu Rev Genet* **46**, 677-700, doi:10.1146/annurev-genet-
546 110711-155522 (2012).
547 39 Meyerson, N. R. & Sawyer, S. L. Two-stepping through time: mammals and
548 viruses. *Trends Microbiol* **19**, 286-294, doi:10.1016/j.tim.2011.03.006 (2011).
549 40 Kosiol, C. *et al.* Patterns of positive selection in six Mammalian genomes. *PLoS*
550 *Genet* **4**, e1000144, doi:10.1371/journal.pgen.1000144 (2008).
551 41 Lander, E. S. *et al.* Initial sequencing and analysis of the human genome. *Nature*
552 **409**, 860-921, doi:10.1038/35057062 (2001).
553 42 Trapnell, C., Pachter, L. & Salzberg, S. L. TopHat: discovering splice junctions
554 with RNA-Seq. *Bioinformatics* **25**, 1105-1111, doi:10.1093/bioinformatics/btp120
555 (2009).
556 43 Trapnell, C. *et al.* Transcript assembly and quantification by RNA-Seq reveals
557 unannotated transcripts and isoform switching during cell differentiation. *Nat*
558 *Biotechnol* **28**, 511-515, doi:10.1038/nbt.1621 (2010).
559 44 Anders, S., Pyl, P. T. & Huber, W. HTSeq--a Python framework to work with
560 high-throughput sequencing data. *Bioinformatics* **31**, 166-169,
561 doi:10.1093/bioinformatics/btu638 (2015).
562 45 Love, M. I., Huber, W. & Anders, S. Moderated estimation of fold change and
563 dispersion for RNA-seq data with DESeq2. *Genome Biol* **15**, 550,
564 doi:10.1186/s13059-014-0550-8 (2014).

565 46 Quinlan, A. R. & Hall, I. M. BEDTools: a flexible suite of utilities for comparing
566 genomic features. *Bioinformatics* **26**, 841-842, doi:10.1093/bioinformatics/btq033
567 (2010).
568 47 Huang, D. W. *et al.* The DAVID Gene Functional Classification Tool: a novel
569 biological module-centric algorithm to functionally analyze large gene lists.
570 *Genome Biol* **8**, R183, doi:10.1186/gb-2007-8-9-r183 (2007).
571 48 Afgan, E. *et al.* The Galaxy platform for accessible, reproducible and
572 collaborative biomedical analyses: 2016 update. *Nucleic Acids Res* **44**, W3-W10,
573 doi:10.1093/nar/gkw343 (2016).
574 49 Schmittgen, T. D. & Livak, K. J. Analyzing real-time PCR data by the comparative
575 C(T) method. *Nat Protoc* **3**, 1101-1108 (2008).
576

577 Acknowledgements

578 This work was supported by the Northwestern University NUSeq Core Facility, High
579 Throughput Analysis Laboratory and Quest High Performance Computing Facility. We
580 are grateful to Adam J. Hockenberry and members of the Horvath lab for critical
581 comments and helpful suggestions, and to Dr. Christian Stehlik and Dr. Lucia Maria de
582 Almeida for providing THP-1 cells. Supported by NIH grants AI073919, AI50707, and
583 GM111652 to C.M.H. R.M. was supported by a pre-doctoral fellowship from the NIH
584 Training Program in Viral Replication T32AI60523.
585

586 Author Contributions

R.M. and C.M.H. designed the study and wrote the manuscript; R.M. conducted the experiments and analysis. All authors read and approved the final manuscript.

Additional Information

Competing Interests: The authors declare that they have no competing interests.

Accession codes: RNA-sequencing data is available in the GEO database under study GSE115266.

Figures & Tables

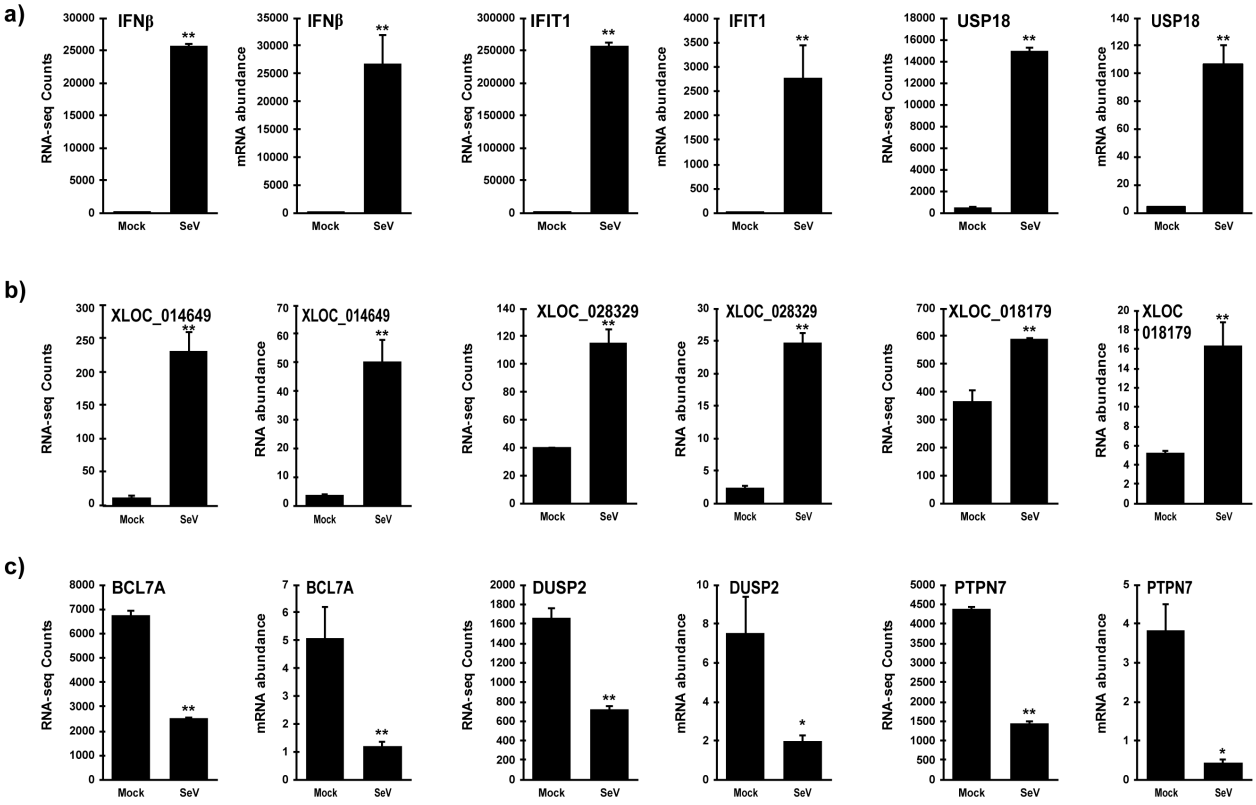

Figure 1 - Validation of differential gene expression induced by Sendai virus infection.

Namalwa cells were infected with Sendai virus for 6 hours and total RNA was analyzed by RNA-sequencing or by RT-qPCR in independent samples. For each indicated RNA, RNA-sequencing counts are plotted on the graph on the left and RNA abundance from RT-qPCR on the right. Expression of virus-induced a) previously-annotated genes and b) previously-unannotated RNAs and c) virus-suppressed genes was validated. RNA abundance data is representative of ≥ 2 replicate experiments and is shown normalized to GAPDH expression. Bars indicate average values of technical replicates (n=3) with

606 error bars representing standard deviation. Statistical analysis was done using a two-
607 tailed Student's *t*-test for RT-qPCR measurements (* p-value < 0.05, ** p-value < 0.005)
608

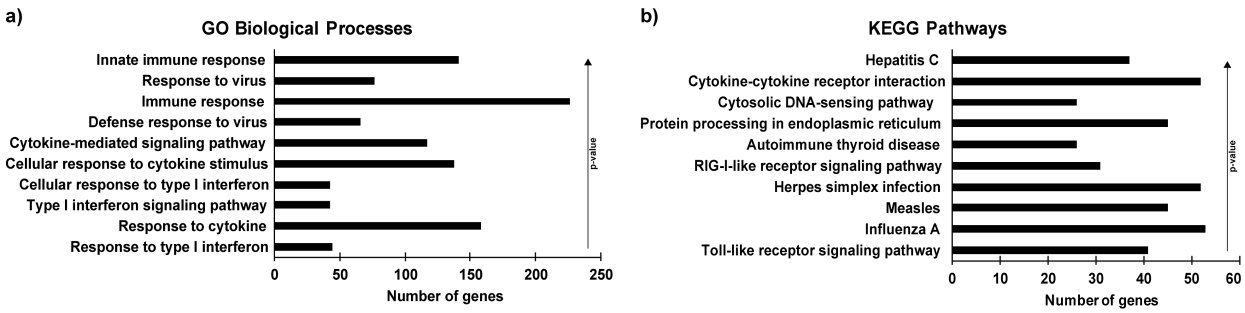

609

610 **Figure 2 - Graphical representation of functional enrichment analysis of Sendai**
611 **virus-induced RNAs.**
612 Sendai virus-induced previously-annotated RNAs were analysed using DAVID to
613 determine enriched a) GO biological processes and b) KEGG pathways. The top 10
614 most significant terms in each analysis are shown here in rank order by p-value. Bars
615 represent number of virus-induced RNAs mapping to each term.
616

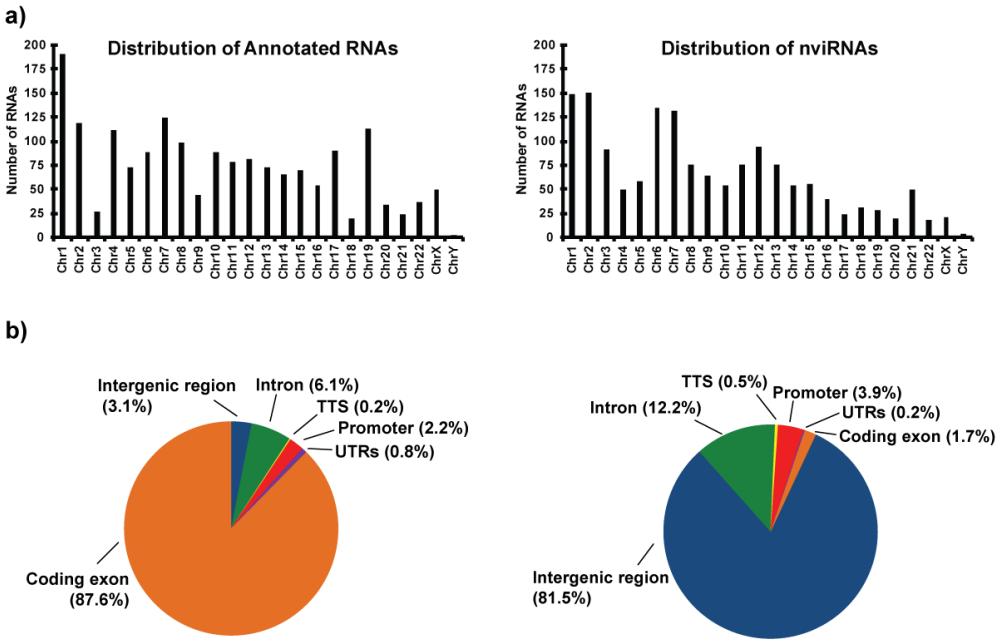

Figure 3 - Comparison of genomic distribution of Sendai virus-induced previously-annotated RNAs and nviRNAs.

a) Bar graphs represent the number of virus-induced previously-annotated RNAs (left) and nviRNAs (right) identified on each chromosome. b) Pie charts illustrate genomic feature distribution of previously RefSeq-annotated RNAs (left) and nviRNAs (right). RNAs are mapped to one of six annotation categories: promoters, transcriptional termination sites (TTS), exons, intergenic regions, introns, and untranslated regions (UTRs; includes 5' and 3' UTRs), with the percentage of sites corresponding to each category displayed in parentheses near the label.

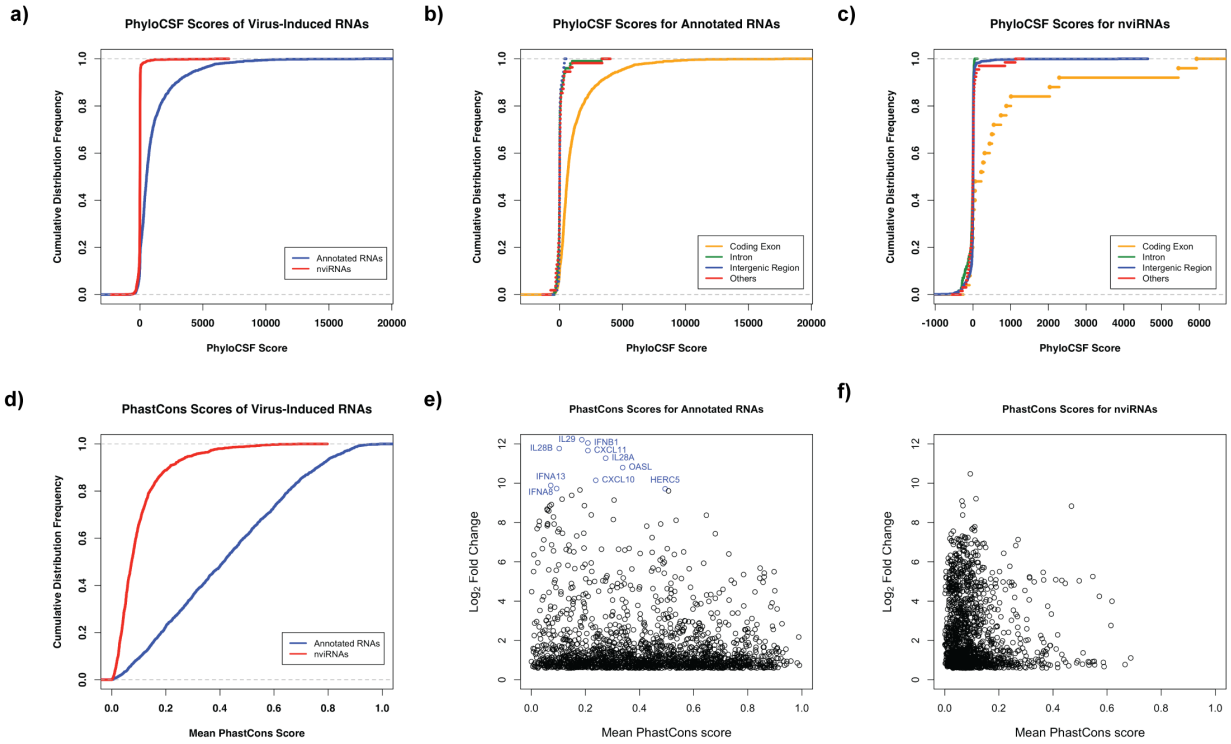

628

629 **Figure 4 - Comparison of protein coding potential and vertebrate sequence**
630 **conservation of Sendai virus-induced previously-annotated RNAs and nviRNAs.**
631 a) The cumulative distribution frequency of PhyloCSF scores for previously-annotated
632 RNAs (blue) and nviRNAs (red). b) The cumulative distribution frequency for RNAs
633 mapping to the different genomic feature annotations for previously RefSeq-annotated
634 RNAs and c) nviRNAs. The different genomic feature annotations include: coding
635 exons (orange), intergenic regions (blue), introns (green), and promoters, transcriptional
636 termination sites, and UTRs (all grouped together; red). d) The cumulative distribution
637 frequency of the mean PhastCons score for the previously-annotated RNAs (blue) and
638 nviRNAs (red). The mean PhastCons score for each RNA is plotted against the $\log_2$
639 fold change in expression after Sendai virus infection for e) previously-annotated RNAs
640 and f) nviRNAs. The 10 most highly-induced previously-annotated RNAs are labeled in
641 blue in e).

642

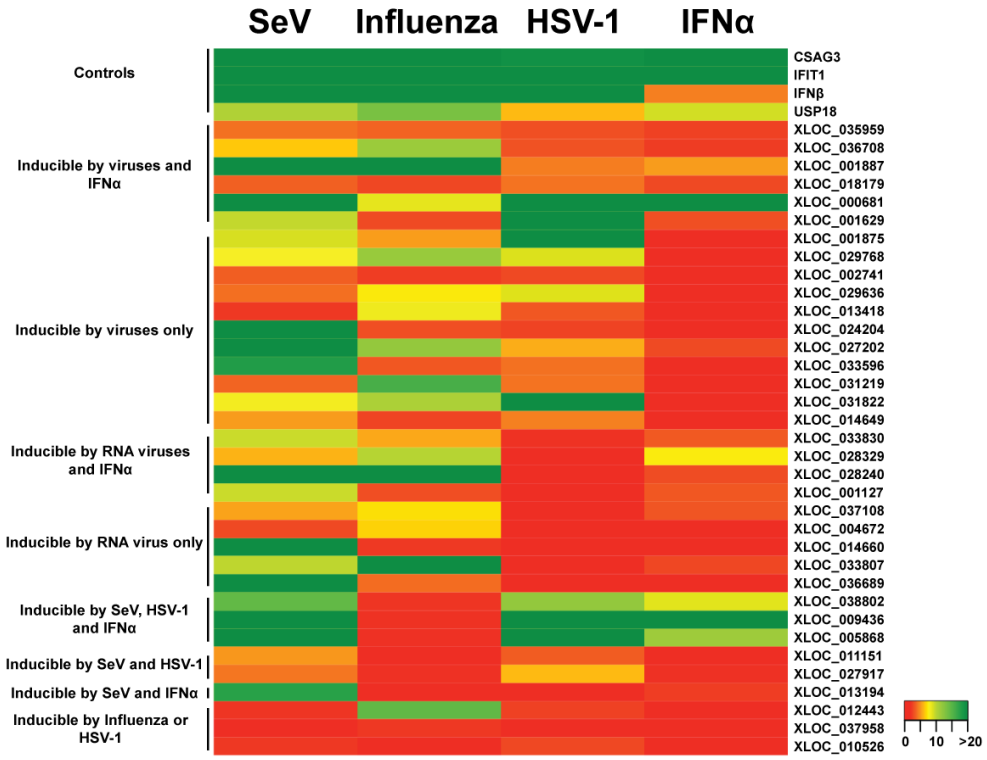

643

644 **Figure 5 - Classification of nviRNA expression in Namalwa cells from various**

645 **stimuli.**

646 Total RNA from Namalwa cells infected with 5 pfu/cell for 10 hours of Sendai virus

647 (SeV), influenza A virus, or HSV-1 or directly treated with 1000 U/mL of IFNα for 6 hours

648 was analyzed by RT-qPCR. Heat map indicates expression of each RNA after infection

649 or treatment with IFNα. Average values (n=3) of fold change are reported normalized to

650 GAPDH expression.

651

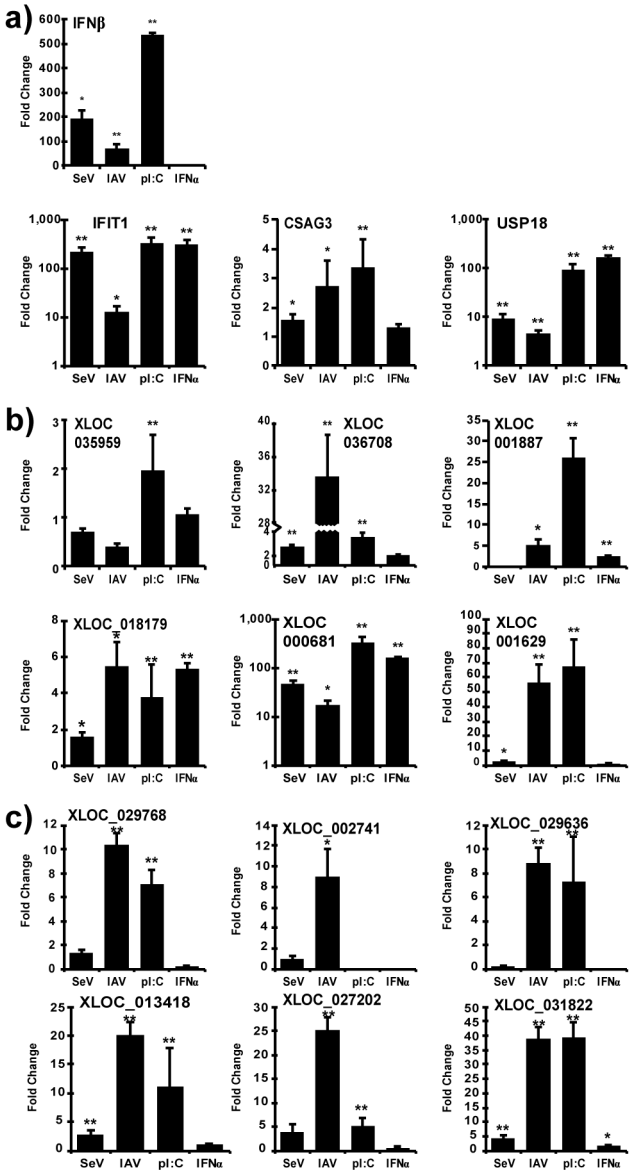

Figure 6 - nviRNA expression in 2fTGH cells.

Total RNA from 2fTGH cells infected with 5 pfu/cell Sendai virus (4 hours) or influenza A virus (IAV;10 hours), or transfected with synthetic dsRNA polyI:C (pI:C; 6 hours), or directly treated with IFNα (6 hours) was analyzed by RT-qPCR. Gene-specific primers were used for a) control genes, b) nviRNAs inducible by viruses and IFNα in Namalwa cells and c) nviRNAs only inducible by viruses in Namalwa cells. Data is representative of ≥2 replicate experiments and is shown normalized to GAPDH expression. Bars

660 indicate average values of technical replicates (n=3) with error bars representing
661 standard deviation. Statistical analysis was done using a two-tailed Student's *t*-test (* p-
662 value < 0.05, ** p-value < 0.005).
663

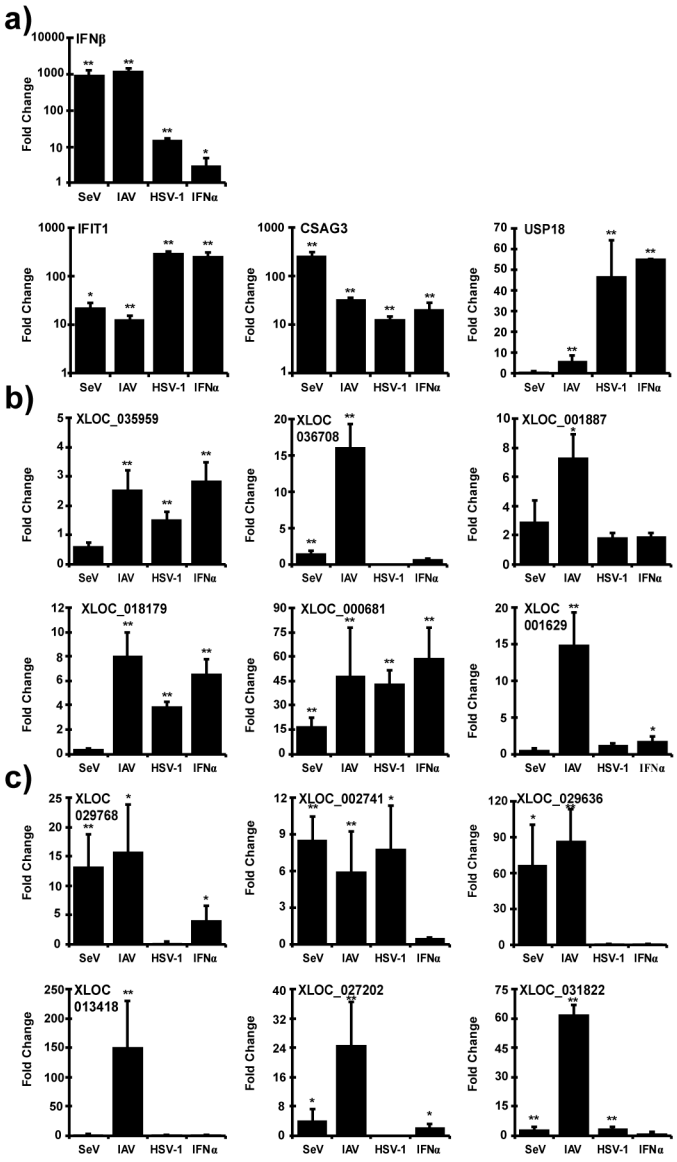

664

665 **Figure 7 - nviRNA expression in THP-1 cells.**

666 Total RNA from THP-1 cells infected with 5 pfu/cell Sendai virus (4 hours), influenza A
667 virus (IAV; 10 hours) or HSV-1 (10 hours) or directly treated with IFNα (6 hours) was

analyzed by RT-qPCR. Gene-specific primers were used for a) control genes, b) nviRNAs inducible by viruses and IFNα in Namalwa cells and c) nviRNAs only inducible by viruses in Namalwa cells. Data is representative of ≥2 replicate experiments and is shown normalized to GAPDH expression. Bars indicate average values of technical replicates (n=3) with error bars representing standard deviation. Statistical analysis was done using a two-tailed Student's *t*-test (* p-value < 0.05, ** p-value < 0.005).

Table 1 – The top 10 highly virus-induced previously-annotated RNAs.

Gene	Log_2 fold change	FDR	PhastCons mean score
IL29	12.21 ± 0.41	3.34E-191	0.187
IFNβ	12.05 ± 0.37	9.06E-229	0.209
IL28β	11.77 ± 0.40	1.33E-186	0.103
CXCL11	11.66 ± 0.34	7.83E-250	0.209
IL28α	11.27 ± 0.42	3.42E-153	0.275
OASL	10.80 ± 0.19	0.00E+00	0.338
CXCL10	10.15 ± 0.13	1.39E-168	0.238
IFNα13	9.89 ± 0.45	0.00E+00	0.072
IFNα8	9.73 ± 0.45	1.17E-106	0.094
HERC5	9.72 ± 0.38	4.91E-102	0.495

677 **Table 2 – Summary of nviRNA expression in various cell types.**

	2fTGH				HeLa					A549				THP-1			
RNA	**IFNα**	**SeV**	**IAV**	**pIC**	**IFNα**	**SeV**	**IAV**	**pIC**	**HSV-1**	**IFNα**	**SeV**	**IAV**	**pIC**	**IFNα**	**SeV**	**IAV**	**HSV-1**
CSAG3	-	-	+	+	+	+	+	+	+	+	+	+	+	+	+	+	+
IFIT1	+	+	+	+	+	+	+	+	+	+	+	+	+	+	+	+	+
IFNβ	-	+	+	+	+	+	+	+	+	+	+	+	+	+	+	+	+
USP18	+	+	+	+	+	+	-	+	+	+	+	+	+	+	-	+	+
XLOC_035959	-	-	-	+	+	-	-	+	-	+	-	+	+	+	-	+	-
XLOC_036708	-	+	+	+	-	-	+	+	+	-	-	+	+	-	-	+	-
XLOC_001887	+	-	+	+	-	-	-	-	-	-	-	+	+	-	-	+	-
XLOC_018179	+	+	+	+	-	-	-	+	-	+	-	+	+	+	-	+	+
XLOC_000681	+	+	+	+	+	+	+	+	+	+	+	+	+	+	+	+	+
XLOC_001629	-	+	+	+	+	-	+	+	+	-	+	+	+	-	-	+	-
XLOC_001875	-	-	-	-	-	-	-	-	-	-	-	-	-	-	-	-	-
XLOC_029768	-	-	+	+	+	-	+	+	+	-	-	-	-	+	+	+	-
XLOC_002741	-	-	+	-	+	-	+	+	-	-	-	+	+	-	+	+	+
XLOC_029636	-	-	+	+	-	-	-	+	-	-	+	+	+	-	+	+	-
XLOC_013418	-	+	+	+	-	-	+	+	+	-	-	+	+	-	-	+	-
XLOC_024204	-	-	-	+	-	-	-	-	-	-	-	-	-	-	-	-	-
XLOC_027202	-	-	+	+	+	+	+	+	-	-	+	+	+	+	+	+	-
XLOC_033596	-	-	-	-	-	-	-	-	-	-	-	-	-	-	+	+	+
XLOC_031219	-	-	+	+	-	-	-	+	-	-	-	+	+	-	-	-	-
XLOC_031822	+	+	+	+	+	-	+	+	+	+	+	+	+	-	+	+	+
XLOC_014649	-	-	-	+	-	-	-	+	-	-	-	-	-	-	-	-	-

678